[18] G. Lu, W. Li, J. Yao, G. Zhang, B. Yang, J. Shen, *Adv. Mater.* **2002**, *14*, 1049.
[19] A. Baba, R. C. Advincula, W. Knoll, in *Novel Methods to Study Interfacial Layers* (Eds: D. Möbius, R. Miller), Elsevier Science, Studies in Interface Science, New York **2001**, Vol. 11, p. 55.
[20] A. Baba, R. C. Advincula, W. Knoll, *J. Phys. Chem. B* **2002**, *106*, 1581.
[21] C. Xia, R. Advincula, A. Baba, W. Knoll, *Langmuir* **2002**, *18*, 3555.
[22] A. Baba, M.-K. Park, R. C. Advincula, W. Knoll, *Langmuir* **2002**, *18*, 4648.

Ruthenium Oxide Nanotube Arrays Fabricated by Atomic Layer Deposition Using a Carbon Nanotube Template

By *Yo-Sep Min*,* *Eun Ju Bae*, *Kwang Seok Jeong*, *Young Jin Cho*, *Jung-Hyun Lee*, *Won Bong Choi*, and *Gyeong-Su Park*

Since the discovery of carbon nanotubes (CNTs),[1] this new carbon allotrope has attracted a great deal of attention because of its nanoscale hollow tubular structure and potential applications. CNT arrays can be applied to various functional nanodevices, such as actuators,[2] nanotransistors,[3] field emitters,[4] and gas sensors.[5] Recently, syntheses of other inorganic nanotubes have mainly focused on compounds possessing graphite-analogue layered structures such as Group 6 chalcogenides (WS_2, MoS_2) and boronitride (BN),[6] since high-temperature processes similar to the CNT synthesis method can be used to prepare their crystalline nanotubes. On the other hand, most oxide nanotubes, such as TiO_2, SiO_2, Al_2O_3, ZrO_2, and V_2O_5, have been prepared using templating agents.[7] Recently, CNTs have been also used as a template to fabricate other nanoscale materials by filling, coating, confined reaction, and substitution reaction.[8]

To our knowledge, no inorganic nanotubes or their arrays have been fabricated at temperatures below 400 °C by chemical vapor deposition (CVD), which is more compatible with current device fabrication processes. Here we report the first successful fabrication of a hollow nanotube array of ruthenium oxide on a silicon wafer by atomic layer deposition (ALD), which is a special modification of CVD for self-limiting film growth.[9] In ALD, an appropriate precursor vapor and a reaction gas are alternately pulsed onto a substrate. The reaction chamber is purged with an inert gas between the pulses of the precursor vapor and the reaction gas. All the process steps are performed at low temperatures, normally lower than 400 °C, to avoid thermal decomposition of the chemisorbed source molecules. The principle of the process is that film deposition occurs through the surface reaction between the reaction gas and the saturated surface monolayer of source molecules. Consequently, the thickness of the film can be accurately controlled by the number of process cycles, each of which consists of source gas pulse–purge–reaction gas pulse–purge.

In this research, CNT arrays on porous anodic aluminum oxide (AAO) were used as a template to grow Ru thin films by ALD. The Ru-coated CNT arrays were then heated in an oxygen atmosphere to remove the CNT template. After ashing of the CNTs, ruthenium oxide nanotube arrays were obtained by the oxidation of ruthenium and the removal of CNTs.

To prepare a removable template of CNT arrays, we used a procedure similar to that mentioned in a previous report.[10] Ordered hole arrays of AAO, of ~35 nm pore diameter and ~10^{10} cm^{-2} pore density, were fabricated by a two-step aluminum anodization. Scanning electron microscopy (SEM) and dynamic force microscopy (DFM) were used to image the ordered CNT arrays, showing that the exposed heights and the inner diameters of the CNTs are about 70–100 nm and 30–50 nm, respectively (Figs. 1a,d). As previously reported,[10] the CNTs are hollow, multi-walled, and highly defective, since they were obtained without a catalyst during their growth.

Ru thin films were first deposited on a SiO_2/Si wafer to investigate the process window of ALD using $Ru(od)_3$/*n*-butylacetate solution (0.1 M) (here od is octane-2,4-dionate)[11] and oxygen gas. The process window of ALD appeared in the temperature region from 325–375 °C. Figure 2a shows a typical plateau of ALD growth rate that is nearly independent of the deposition temperature. The $Ru(od)_3$ dose for saturated adsorption is three or more injections in a cycle (~0.03 mL), as shown in Figure 2b. When the dose is insufficient, the deposition rate increases with the source injection frequency. Above a dose of three times per cycle, the growth rate is independent of the $Ru(od)_3$ dose, since the growing surface is already saturated with $Ru(od)_3$. Ru ALD is the first report on metal thin film growth by ALD using a metal β-diketonate precursor. Since β-diketonate ligands usually decomposed in an oxygen atmosphere, ALD with a metal β-diketonate precursor and oxygen gas generally results in metal oxide films.[12] However, ALD with $Ru(od)_3$ and oxygen gas surprisingly gives a metallic Ru thin film, instead of ruthenium oxide.

On the templates of CNT arrays, Ru thin films (~6 nm) were coated at 300 °C by ALD using $Ru(od)_3$/*n*-butylacetate solution and oxygen gas. This deposition temperature, below the temperature window for ALD, was chosen to avoid the oxidation of CNTs during the ALD process. To easily remove the CNT templates, we chose non-saturated process conditions caused by an insufficient supply of precursors. Therefore, the $Ru(od)_3$ dose was restricted to one injection per cycle (~0.01 mL) to induce an non-saturated adsorption, even though saturated adsorption could be obtained by injecting $Ru(od)_3$ solution three or more times in a cycle (~0.03 mL).

The SEM image in Figure 1b shows that the Ru films were deposited on the surface of CNTs that protruded from the

[*] Y.-S. Min, E. J. Bae, K. S. Jeong, Y. J. Cho, Dr. J.-H. Lee, Dr. W. B. Choi
Materials and Devices Laboratory
Samsung Advanced Institute of Technology
PO Box 111, Suwon 440-600 (Korea)
E-mail: ysmin@sait.samsung.co.kr
Dr. G.-S. Park
Analytical Engineering Center
Samsung Advanced Institute of Technology
PO Box 111, Suwon 440-600 (Korea)

 DOI: 10.1002/adma.200304452

ADVANCED MATERIALS

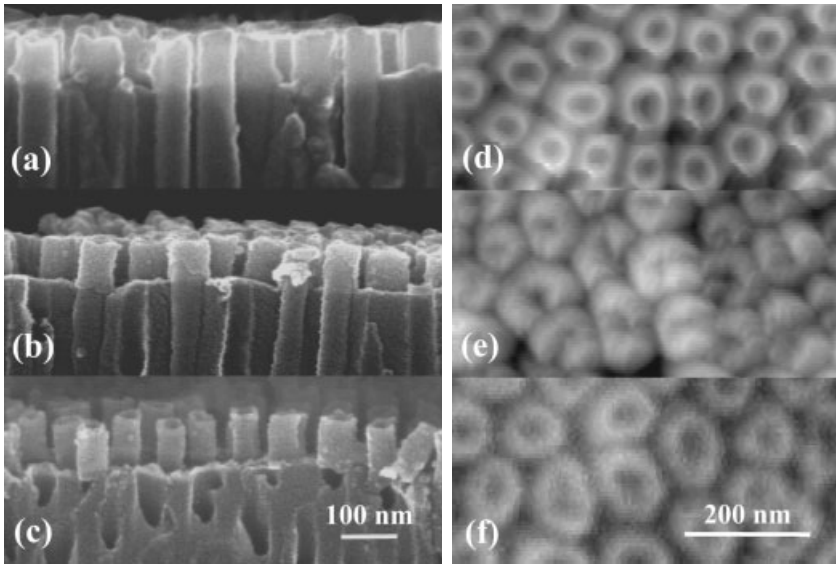

Fig. 1. SEM (a–c) and DFM (d–f) images of CNT array (a,d), Ru-coated CNT array (b,e), and RuO_2 nanotube array (c,f).

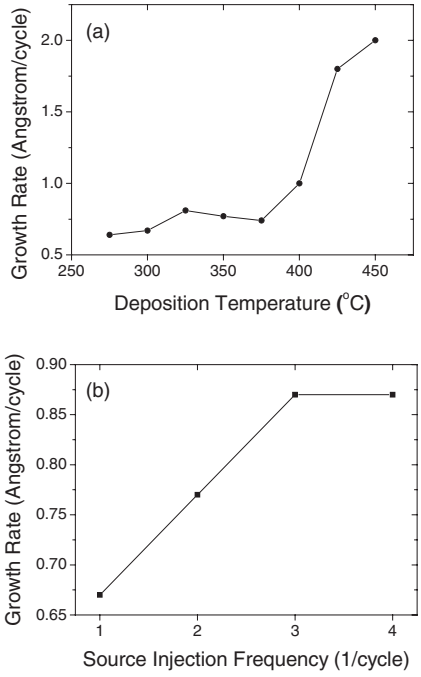

Fig. 2. Dependence of Ru film growth rate on deposition temperature (a) and source injection frequency (b). This result was obtained from Ru films grown on SiO_2/Si substrates under the same conditions as the Ru ALD on a CNT array.

porous AAO matrix. The inner diameters of the nanotubes were reduced by the growth of Ru film inside the CNTs, as demonstrated in the DFM image of the Ru-coated CNT arrays (Fig. 1e). High-resolution transmission electron microscopy (HR-TEM) (Fig. 3a) also indicates that Ru films grew on the inner and outer surfaces of CNTs. The digital diffractogram of the framed area shows the presence of a spot due to the (101) plane of polycrystalline Ru films as shown in the inset of Figure 3a. However, the density of Ru films on the outer surfaces of CNTs is different from those on inner surfaces, since the Ru films were deposited under non-saturated

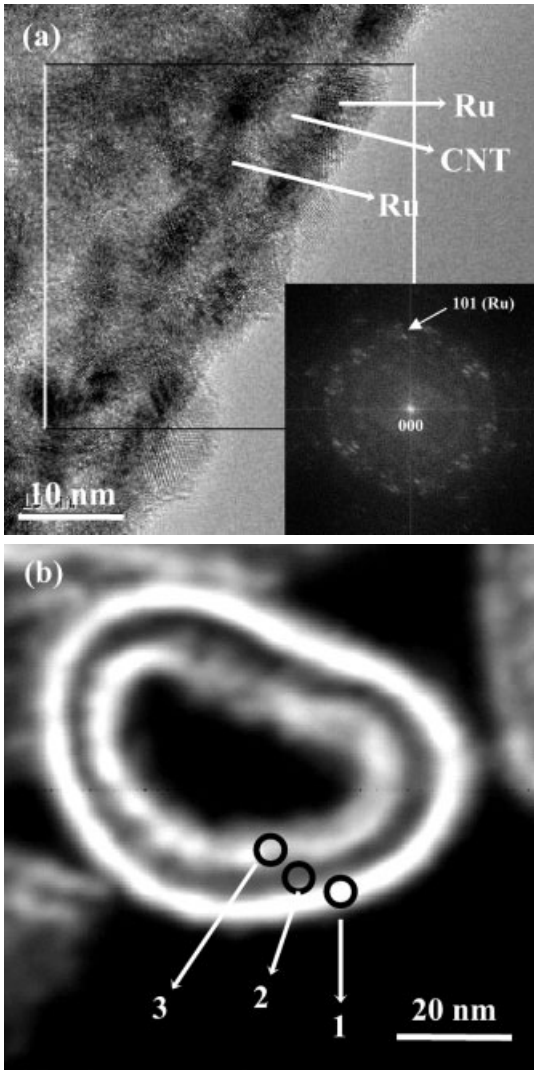

Fig. 3. HR-TEM image (a) and *Z*-contrast image (b) of a Ru-coated CNT. Inset: The digital diffractogram of the framed area of a Ru-coated nanotube. Positions 1–3 denote outer Ru film (1), CNT (2), and inner Ru film (3).

conditions owing to the insufficient supply of $Ru(od)_3$. The *Z*-contrast image in Figure 3b clearly shows that the outer Ru film is denser than the inner one. Such a density discrepancy of Ru films is possibly due to the different adsorption behavior of $Ru(od)_3$ molecules between the inner and outer surfaces. In other words, the outer surfaces of nanotubes can more easily adsorb $Ru(od)_3$ than the inner ones, because the outer surfaces are more exposed to the $Ru(od)_3$ vapor.

Analysis by energy dispersive spectroscopy (EDS) (Table 1) of the positions denoted in Figure 3b also indicates that the outer (1) and inner (3) films on CNTs (2) are ruthenium. Although $Ru(od)_3$ is a β-diketonate complex including oxygen in the ligand, the deposited films mainly consist of ruthenium atoms without oxygen atoms (1) or with a small amount of them (3). More carbon and oxygen atoms were detected in the inner film (3) than in the outer one, because the gaseous by-products from the inner surface of nanotubes can be purged less efficiently. This is another reason for the density discrepancy mentioned above.

Table 1. Results of TEM-EDS in positions denoted in Figures 3 and 4; the values are given in counts of the characteristic X-ray of each element. Blanks (–) represent negligible signal due to very low signal-to-noise ratios.

Characteristic X-ray (Energy, *hv* [keV])	Ru/CNT (Fig. 4)			RuO_2 (Fig. 5)	
	1	2	3	4	5
C Kα (0.282)	32	117	64	12	22
O Kα (0.523)	–	14	18	59	59
Al Lα (1.487)	–	–	–	116	31
Ru Kα (2.588)	110	33	116	8	99

To remove carbons from the Ru-coated CNT arrays by ashing, the specimens were heated at 500 °C in an oxygen atmosphere for 1 h. Generally, CNTs can be oxidized to CO_2 gas in an oxygen atmosphere at a temperature above 400 °C, because they consist of carbon atoms connected to each other by covalent bonds. After the CNTs had been burnt away, new inorganic nanotube arrays were subsequently fabricated as shown in Figure 1c. The empty AAO pores in the cross section of the new nanotube arrays reveal that CNTs were nearly completely removed from the pores by the ashing. The inner diameters of the new nanotubes were increased by the removal of carbon as shown in the DFM image of Figure 1f. We speculate that the removal path of carbon has relevance to the sparse microstructure of the inner side Ru films.

The HR-TEM image (Fig. 4a) of the new nanotube also shows that nearly all carbon was removed from the Ru-coated CNT, and that the surface morphology was roughened after heat treatment in an oxygen atmosphere. In Table 1 and Figure 4b, TEM-EDS results from the new nanotubes also reveal that the new nanotubes (5) mainly consist of ruthenium and oxygen atoms with small amounts of carbon residue. Even though aluminum atoms are detected in the nanotubes (5), this may be due to the AAO matrix in consideration of the EDS result of position 4. In other words, we have succeeded in preparing ruthenium oxide nanotube arrays by the template method. The diffractogram in the inset of Figure 4a also

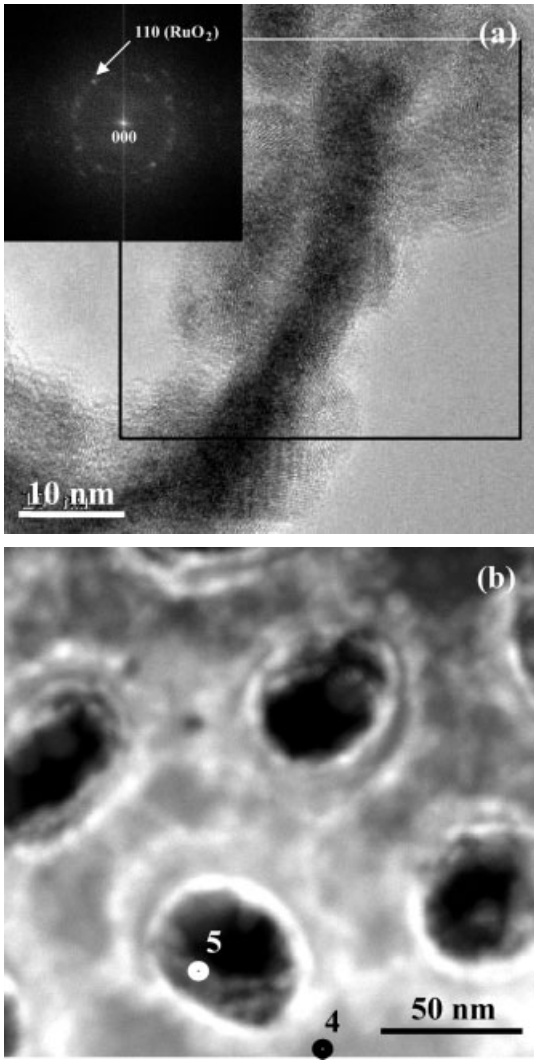

Fig. 4. HR-TEM image (a) and *Z*-contrast image (b) of a RuO_2 nanotube. Inset: The digital diffractogram of the framed area of a RuO_2 nanotube. Positions 4 and 5 denote AAO matrix (4) and RuO_2 nanotube (5).

indicates the presence of a spot corresponding to the (110) plane of RuO_2. During the heat treatment of the Ru-coated CNT arrays in oxygen atmosphere, the carbons placed between Ru films are burned away and removed from nanotubes. The inner and outer Ru films are stuck together and roughened by ruthenium oxide formation.

In conclusion, ruthenium oxide nanotube arrays were successfully fabricated by ALD using CNT arrays as a removable template. ALD with $Ru(od)_3$ and oxygen gas resulted in a metallic Ru thin film on the CNT arrays. The Ru-coated CNT arrays were then heated in an oxygen atmosphere to remove the CNTs. Ruthenium oxide nanotube arrays were subsequently obtained by the oxidation of the Ru films during the removal process of the CNT template. The CNT-template ALD method can be used to fabricate other inorganic nanotube arrays as well as ruthenium oxide, if a combination of ALD precursors and reaction gas is available that does not degrade the CNT template during ALD. Nowadays, even

ADVANCED MATERIALS

though ALD is mainly applied to high-*k* dielectric ultra-thin films for gate oxides of field-effect transistors because of the low deposition rate, it is a useful tool for nanostructure fabrication as demonstrated in this study.

Experimental

AAO Fabrication: An ordered hole array of AAO, pore diameter ~35 nm and pore density ~10^{10} cm^{-2}, was fabricated by aluminum anodization. Al thin film (500 nm) was sputtered on a silicon wafer and then oxidized in a 0.3 M oxalic acid solution at 16 °C under a constant voltage of 40 V. The pore diameter of the AAO was increased in 0.1 M phosphoric acid solution.

CNT Growth: For CNT growth on AAO by CVD, the AAO/Si substrate was first heated at 600 °C in a nitrogen atmosphere. The CNTs were then grown inside the pores by catalytically pyrolyzing acetylene for 20 min using 10 % acetylene in nitrogen carrier gas (100 sccm). The resulting specimen was ion-milled to remove residual amorphous carbon from the template surface and the CNTs were partially exposed by etching the alumina matrix using a mixture of phosphoric acid and chromic acid.

Ru ALD: Metallic Ru thin films (~6 nm) were coated on the CNT array by ALD using $Ru(od)_3$/*n*-butylacetate solution (0.1 M) (od = octane-2,4-dionate) and oxygen gas. $Ru(od)_3$ solution was kept in a canister pressurized with argon fitted with a liquid injector. The injector was connected to a vaporizer, which was attached to a reaction chamber containing the CNT template. When the injector was turned on, about 0.01 mL $Ru(od)_3$ solution was injected and carried by Ar gas (150 sccm) to the vaporizer, which was kept at 200 °C. The valves for $Ru(od)_3$ vapor and oxygen gas (100 sccm) were alternately opened for 2 s with an interval of 3 s to purge volatile byproducts and any excess reactants in the reaction chamber with Ar (300 sccm). The working pressure was regulated to about 1 torr in every step by an automatic valve for 70 cycles.

Removal of CNT Templates: To remove carbon nanotube templates by ashing, the Ru-coated CNT array was heated at 500 °C in an oxygen flow of 100 sccm (1 torr) for 1 h.

Analytical Method: DFM images were obtained with a dynamic force microscope in non-contact mode (SPA 500, Seiko Instruments Inc.). All DFM experiments were performed in air at room temperature. The HR-TEM images, EDS spectra, and annular dark-field scanning transmission electron microscope (ADF-STEM) images were obtained by a TECNAI-UT30 microscope equipped with a Schottky-type field emission gun operating at 300 kV.

Received: September 23, 2002
Final version: March 19, 2003

[1] S. Iijima, *Nature* **1991**, *354*, 56.
[2] a) P. Poncharal, Z. L. Wang, D. Ugarte, W. A. de Heer, *Science* **1999**, *283*, 1513. b) R. H. Baughman, C. Cui, A. A. Zakhidov, Z. Iqbal, J. N. Barisci, G. M. Spinks, G. G. Wallace, A. Mazzoldi, D. D. Rossi, A. G. Rinzler, O. Jaschinski, S. Roth, M. Kertesz, *Science* **1999**, *284*, 1340.
[3] a) S. J. Tans, A. R. M. Verschueren, C. Dekker, *Nature* **1998**, *393*, 49. b) W. B. Choi, J. U. Chu, K. S. Jeong, E. J. Bae, J. W. Lee, J. J. Kim, J. O. Lee, *Appl. Phys. Lett.* **2001**, *79*, 3696.
[4] a) Q. H. Wang, A. A. Setlur, J. M. Lauerhaas, J. Y. Dai, E. W. Seelig, R. P. H. Chang, *Appl. Phys. Lett.* **1998**, *72*, 2912. b) S. Fan, M. G. Chapline, N. R. Franklin, T. W. Tombler, A. M. Cassell, H. Dai, *Science* **1999**, *283*, 512.
[5] a) J. Kong, N. R. Franklin, C. Zhou, M. G. Chapline, S. Peng, K. Cho, H. Dai, *Science* **2000**, *287*, 622. b) P. G. Collins, K. Bradley, M. Ishigami, A. Zettl, *Science* **2000**, *287*, 1801.
[6] a) R. Tenne, L. Margulis, M. Genut, G. Hodes, *Nature* **1992**, *360*, 444. b) Y. Feldman, E. Wasserman, D. J. Srolovitz, R. Tenne, *Science* **1995**, *267*, 222. c) E. J. M. Hamilton, S. E. Dolan, C. E. Mann, H. O. Colijin, C. A. McDonald, S. G. Shore, *Science* **1993**, *260*, 659.
[7] a) P. Hoyer, *Langmuir* **1996**, *12*, 1411. b) B. C. Satishkumar, A. Govindaraj, E. M. Vogl, L. Basumallick, C. N. R. Rao, *J. Mater. Res.* **1997**, *12*, 604. c) C. N. R. Rao, B. C. Satishkumar, A. Govindaraj, *Chem. Commun.* **1997**, 1581. d) M. E. Spahr, P. Bitterli, R. Nesper, M. Müller, F. Krumeich, H. U. Nissen, *Angew. Chem. Int. Ed.* **1998**, *37*, 1263. e) P. Hoyer, *Adv. Mater.* **1996**, *8*, 857.
[8] a) P. M. Ajayan, O. Stephan, P. Redlich, C. Colliex, *Nature* **1995**, *375*, 564. b) W. Han, S. Fan, Q. Li, Y. Hu, *Science* **1997**, *277*, 1287. c) W. Han, Y. Bando, K. Kurashima, T. Sato, *Appl. Phys. Lett.* **1998**, *73*, 3085. d) J. Sloan, J. Hammer, M. Zwiefka-Sibley, M. L. H. Green, *Chem. Commun.* **1998**, 347. e) C. J. Brumlik, C. R. Martin, *J. Am. Chem. Soc.* **1991**, *113*, 3174. f) B. C. Satishkumar, A. Govindaraj, M. Nath, C. N. R. Rao, *J. Mater. Chem.* **2000**, 2115.
[9] T. Suntola, *Handbook of Crystal Growth*, Vol. 3 (Ed: D. T. J. Hurle), Elsevier, Amsterdam **1994**, p. 601.
[10] E. J. Bae, W. B. Choi, K. S. Jeong, J. U. Chu, G. S. Park, S. S. Song, I. K. Yoo, *Adv. Mater.* **2002**, *14*, 277.
[11] a) K. Onozawa, A. Masuko, *US Patent 6316064 B1*, **2001**. b) J. H. Lee, J. Y. Kim, S. W. Rhee, D. Y. Yang, D. H. Kim, C. H. Yang, Y. K. Han, C. J. Hwang, *J. Vac. Sci. Technol. A* **2000**, *18*, 2400.
[12] I. K. Igumenov, A. E. Turgambaeva, P. P. Semyannikov, *J. Phys. IV* **2001**, *11*, Pr3-505.

Low-Temperature Fabrication of Highly Crystalline SnO_2 Nanorods**

By *Dong-Feng Zhang*, *Ling-Dong Sun*, *Jia-Lu Yin*, and *Chun-Hua Yan**

Stimulated by their unusual optical, electronic, and chemical properties and their potential uses as nanoscale devices, coupled with the ever-present desire for miniaturization, great efforts have been devoted to synthesizing nanostructured semiconductors.[1–6] The size and morphology of such semiconductors very strongly affect their applications as catalysts, solar cells, light-emitting diodes, biological labeling, and so on.[7–10] SnO_2, a stable and large bandgap semiconductor, is well known for its excellent gas sensitivity.[11] It has also been widely investigated for transistors, electrode materials, and solar cells.[12–14] Several methods have been employed to prepare SnO_2 nanocrystals, including sol–gel,[15] hydrothermal,[16] chemical deposition,[17] magnetron sputtering,[18] and microwave irradiation processes.[19] However, the obtained products are mainly films or nanoparticles. Only a few reports have emerged that target one-dimensional (1D) SnO_2 nanomaterials. Meanwhile, it has been proved that 1D single-crystalline SnO_2 is a good candidate for miniaturized, ultrasensitive gas sensors.[20]

Rutile-structured 1D SnO_2 has been obtained as nanorods ~20–40 nm in width with fairly satisfying uniformity by annealing the precursor mixtures.[21] The aspect ratio and uniformity of the SnO_2 nanorods are further improved by thermal oxidation of Sn/SnO at a higher temperature (>1000 °C), which leads to a remarkable increase in diameter.[22] SnO_2 nanoribbons, thereafter, have also been obtained using an improved rapid oxidation method by programmed temperature ramping, and the diameter was reduced to ~30–150 nm.[23] It is acknowledged that the increased temperature provides bet-

[*] Prof. C. H. Yan, Prof. L. D. Sun, D. F. Zhang, J. L.Yin
State Key Laboratory of Rare Earth Materials Chemistry and Applications and PKU-HKU Joint Lab in Rare Earth Materials and Bioinorganic Chemistry
College of Chemistry and Molecular Engineering
Peking University
Beijing 100871 (P.R. China)
E-mail: chyan@chem.pku.edu.cn

[**] This work is supported by the NSFC (20001002 & 20023005), MOST (G19980613), MOE (the Foundation for University Key Teacher), and the Founder Foundation of PKU. We also thank Dr. R. M. Wang for the characterization of HRTEM.

  DOI: 10.1002/adma.200304899